Field-dependent ac susceptibility of amorphous $(Fe_{1-x}Mn_x)_{75}P_{16}B_6Al_3$: the strongly frustrated regime

1998 J. Phys.: Condens. Matter 10 8535

(http://iopscience.iop.org/0953-8984/10/38/014)

J. Phys.: Condens. Matter **10** (1998) 8535–8552. Printed in the UK PII: S0953-8984(98)94444-7

Field-dependent ac susceptibility of amorphous $(Fe_{1-x}Mn_x)_{75}P_{16}B_6Al_3$: the strongly frustrated regime

Anita G Berndt, H P Kunkel and Gwyn Williams

Department of Physics and Astronomy, University of Manitoba, Winnipeg, MB, Canada, R3T 2N2

Received 19 May 1998, in final form 20 July 1998

Abstract. Detailed measurements of the field- and temperature-dependent ac susceptibility $\chi(H, T)$ of amorphous $(Fe_{1-x}Mn_x)_{75}P_{16}B_6Al_3$ for $x = 0.30$–0.41, a composition regime that has been characterized as strongly frustrated by previous neutron depolarization and electron microscopy studies, are presented. Whereas the $x = 0.41$ specimen appears to exhibit a single paramagnetic–spin-glass transition on cooling, this detailed analysis indicates that samples with $x = 0.30$ and $x = 0.32$ display two transitions. In both latter specimens, $\chi(H, T)$ near the upper transition exhibits a line of maxima which decrease in amplitude but increase in temperature as the field is increased; the locus of these maxima delineates a crossover line consistent with the presence of critical fluctuations accompanying a (continuous) paramagnetic–ferromagnetic transition. At lower temperature the non-linear response of these same two samples exhibits a distinct (but not divergent) anomaly, in contrast to the behaviour reported for specimens with lower values for x. Indeed, for the first time, we report the observation (for the $x = 0.32$ sample) of a more pronounced anomaly in this non-linear behaviour near the *lower*-temperature transition than that observed at the upper transition. On the basis of these new data, a modified phase diagram for the amorphous FeMn system is constructed.

1. Introduction

A recent paper [1] reported the results of detailed measurements, and their analysis, of the field- and temperature-dependent alternating-current (ac) susceptibility $\chi(H, T)$ of amorphous $(Fe_{1-x}Mn_x)_{75}P_{16}B_6Al_3$. This study focused on the composition range $0.235 \leqslant x \leqslant 0.26$, which had been categorized previously as one which exhibited the effects of 'weak frustration'. Specifically, the interpretation of electron microscopy studies [2] and neutron depolarization measurements [3] suggested that throughout this concentration region this system displayed a domain size which did not change appreciably at low temperatures, contrasting markedly with the behaviour reported for larger x $(0.3 \leqslant x)$. This result was considered to be significant since measurements of the temperature dependence of the low-field magnetization of samples with $0.235 \leqslant x \leqslant 0.26$ (reference [3] and references listed therein) revealed features that were qualitatively consistent with those attributed to the presence of sequential magnetic transitions; namely, with decreasing temperature the low-field magnetization increased rapidly as the paramagnetic-to-ferromagnetic transition (at T_c) was approached from above, then passed through a weakly temperature-dependent plateau region before decreasing abruptly at the temperature T_{xy} taken as designating the boundary between the ferromagnetic phase and the (transverse) re-entrant spin-glass phase. Such a sequence is predicted to occur by models [4, 5] of magnetic systems with exchange interactions which vary in magnitude and sign and when the mean value of the corresponding

0953-8984/98/388535+18$19.50

distribution ($\bar{J}_0$) is positive and comparable to the width ($\bar{J}$), i.e. $\bar{J}_0 \geqslant \bar{J}$. It was argued that the results of the microscopy and depolarization studies removed the possibility that those features characterizing the second (lower-temperature) transition originated from rapid variations in domain size, and hence the parameters which influence such variations. Thus the (re-entrant) ground state, and the transition separating it from the higher-temperature ferromagnetic state, *might* be categorized as one associated with true (replica) symmetry breaking in this system.

The detailed analysis [1] of $\chi(H, T)$ argued against this latter possibility. While these latter data confirmed the occurrence of a paramagnetic-to-ferromagnetic transition—$\chi(H, T)$ exhibited a maximum which moved upwards in temperature above T_c and decreased in amplitude as H increased, in agreement with the predictions of the static scaling law [6] (and discussed in more detail below)—various lower-temperature features (all potential candidates for delineating the re-entrant phase boundary) failed to satisfy the detailed predictions made by vector models for the so-called Gabay–Toulouse (GT) line [7] (associated with replica symmetry breaking resulting from the initial establishment of transverse spin-glass order coexisting with longitudinal ferromagnetic order, and believed to be accompanied by 'weak' irreversible behaviour) or the de Almeida–Thouless (AT) line [8] (at which a crossover to 'strong' irreversibility is thought to occur). More importantly, in our opinion, was the failure to observe an anomaly in the non-linear response in this low-temperature region; such an anomaly—while being an Ising model prediction [9]—has, nevertheless, been reported for several potentially re-entrant systems, including [10, 11] amorphous **Fe**Zr and (**Pd**Fe)Mn. The behaviour of $\chi(H, T)$ in these weakly frustrated systems was therefore judged to be *inconsistent* with the presence of a true re-entrant transition, and it was suggested that the observed response was more likely to originate from sources such as thermally activated blocking [12] or the breakdown of the ferromagnetic state suggested, for example, in the random-field (RF) approach [13].

Here we report new results of a corresponding investigation of $(Fe_{1-x}Mn_x)_{75}P_{16}B_6Al_3$ for samples with $x = 0.30$, 0.32 and 0.41, revealing markedly different behaviour. This composition range has been designated—following depolarization studies [3]—as strongly frustrated (having a domain size which decreases at low temperature), with the behaviour of specimens with the latter composition approaching that of a non re-entrant, true spin-glass. In contrast to the behaviour reported at lower values for x, we find a distinct—though not divergent—anomaly in the non-linear response of the $x = 0.30$ and 0.32 samples at low temperature, consistent with the presence of a re-entrant ferromagnetic-to-(transverse) spin-glass transition. Indeed, for the $x = 0.32$ specimen we report—for the first time—a more pronounced anomaly in this non-linear response at the *lower*-temperature transition. The reporting of such data appears particularly opportune following our observation of similar structure in preliminary $\chi(H, T)$ data acquired on doped perovskites.

2. Experimental details

The samples studied here were part of the same batch as had been used in the depolarization study [3]; they had been prepared originally by using conventional melt-spinning methods (Bigot and Peynot, Centre d'Etudes de Chimie-Metallurgie, Vitry sur Seine, France) and were subsequently loaned to us by Dr I Mirebeau (Saclay). The in-phase component of the ac susceptibility was recorded continuously using a phase-locked susceptometer [6, 14] with an ac driving field (h_{ac}) of 30 mOe rms at 2.4 kHz and superimposed static biasing fields, H_a, up to 1 kOe. Both types of field were applied along the largest dimension of samples consisting of several electrically isolated strips

of approximate dimensions $15 \times 1 \times 0.05$ mm^3. While relative susceptibility values can be measured with a precision of about one part in 10^4 using this technique, absolute susceptibility values exhibit considerably larger uncertainties. As these samples are quite fragile, they were supplied mounted on masking tape, the removal from which was extremely difficult, complicating accurate determinations of their mass. Furthermore, the demagnetization factors (N) were estimated by approximating each strip by an ellipsoid with principal axes equal to the dimensions given above, and then evaluating the corresponding elliptic integral [15]. This procedure yields an upper limit for N of typically 3×10^{-2} (in mass units). Uncertainties associated with both the above and filling factors combine to render the maximum, absolute susceptibility values in error by up to $\pm 20\%$. Sample temperatures were measured with a (Au + 0.03 at.% Fe)–chromel P thermocouple.

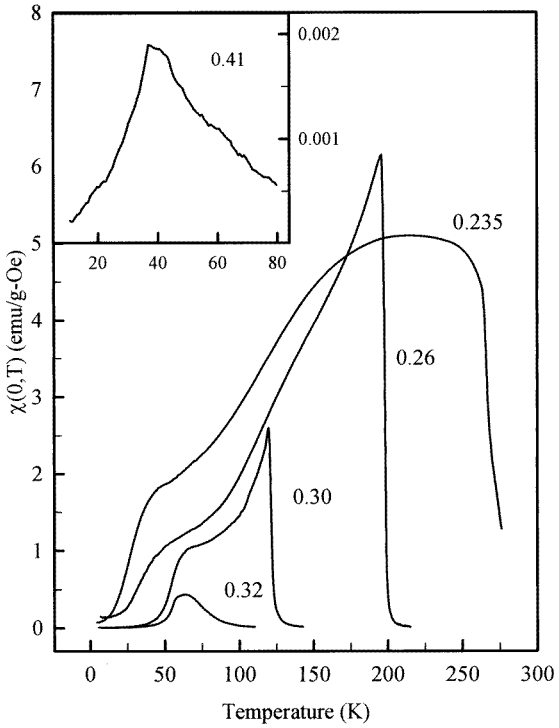

Figure 1. The zero-field ac susceptibility $\chi(0, T)$ (in emu g^{-1} Oe^{-1}), corrected for background and demagnetizing effects, plotted against temperature for several $(Fe_{1-x}Mn_x)_{75}B_{16}P_6Al_3$ samples. The corresponding values of x are marked against the appropriate curves. The inset shows the behaviour of the $x = 0.41$ specimen.

3. Results and discussion

Figure 1 reproduces the temperature dependence of the zero-field ac susceptibility $\chi(0, T)$ for samples with compositions in the range $0.235 \leqslant x \leqslant 0.32$; the corresponding data on the $x = 0.41$ specimen are reproduced in the inset. In agreement with previous conclusions [3], the response of the latter system is typical of a spin-glass rather than

of a potentially re-entrant system; the peak temperature (T_{sg}) is near 38 K while the peak amplitude ($\sim 2 \times 10^{-3}$ emu g^{-1} Oe^{-1}) is over two orders of magnitude smaller than that for the $x = 0.32$ specimen. Here, however, we focus on the detailed response of the potentially re-entrant $x = 0.32$ and $x = 0.30$ systems.

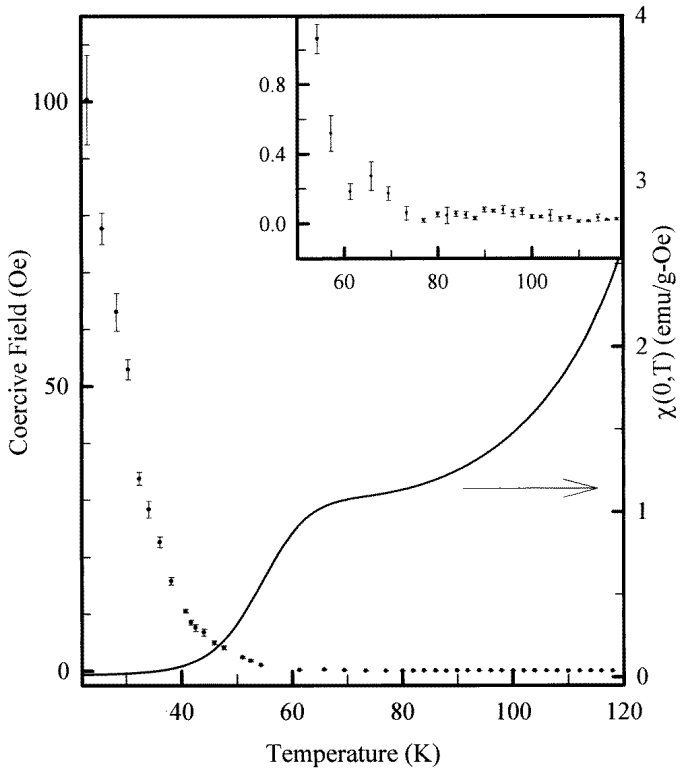

Figure 2. The temperature dependence of the zero-field ac susceptibility $\chi(0, T)$ (in emu g^{-1} Oe^{-1}) and of the coercive field $H_c(T)$ (in Oe) for the $x = 0.30$ sample in the vicinity of the low-temperature shoulder. The inset shows the initial increase in the coercive field at lower temperature in more detail.

Amongst the latter, while the response reproduced in figure 1 for the $x = 0.32$ sample is similar to the variation reported [3] for the low-field ($\sim$20 Oe) magnetization, the zero-field susceptibility of the $x = 0.30$ specimen is quite different; it displays considerably more structure and is similar to that for both the $x = 0.26$ sample and [10] amorphous $Fe_{90}Zr_{10}$. As discussed previously [1, 6, 16], we attribute such difference to the combination of a deliberate choice of samples with *very* low demagnetization factors (this choice has the result that the influence of coercivity/anisotropy effects becomes much more evident [16]) and the presence of a strongly field-dependent initial susceptibility for compositions $x \leqslant 0.3$. Indeed, the trends evident in figure 1 suggest that were it possible to measure the initial susceptibility of the $x = 0.235$ system in still lower ac exciting fields, it *might* display a structure reminiscent of that seen at $x = 0.30$ and $x = 0.26$. To return to the $x = 0.30$ sample, while the susceptibility near the 65 K shoulder is close to the value estimated from the magnetization data [3], the principal (Hopkinson) maximum exceeds the largest reported low-field M/H ratio by a factor of 2–3, but still reaches only some

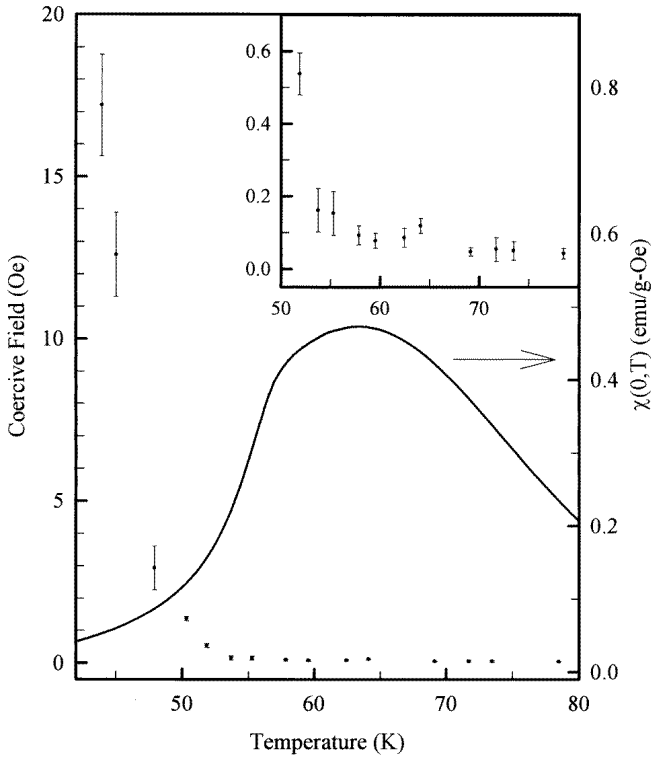

Figure 3. As figure 2, but for the $x = 0.32$ specimen.

6% of the limit set by demagnetization limit constraints for the sample geometry adopted here.

However, before proceeding to discuss the detailed field-dependent ac susceptibility, $\chi(H, T)$, of these samples, and the extent to which features in $\chi(H, T)$ correlate with various model predictions, it is appropriate to consider whether the characteristics of the zero-field response, $\chi(0, T)$—figure 1, on the basis of which claims of re-entrant behaviour are often made—can be linked with so-called technical processes. This has been done by performing 'butterfly loop' measurements, i.e. of $\chi(H_a, T)$ versus the applied field H_a, at various fixed temperatures, from which the corresponding coercive field $H_c(T)$ can be estimated [1, 16]. Figures 2 and 3 confirm that the abrupt decline in $\chi(0, T)$ (near 65 K and 60 K respectively) does correlate with a rapid increase in $H_c(T)$. Nevertheless this result does not prove that the decrease in $\chi(0, T)$ is purely 'technical' in origin, particularly as a closer inspection of the variation in $H_c(T)$ (the insets in these figures) shows that this latter field is close to an order of magnitude larger than the ac driving field (h_{ac}) at the temperature where $\chi(0, T)$ begins to fall. As a rule of thumb, such a decrease is expected to occur (if the effect arises from technical sources) when $H_c(T)$ and h_{ac} are comparable. Figures 2 and 3 do, however, confirm that these lower-temperature features in $\chi(0, T)$ are associated with increased hysteretic—that is, irreversible behaviour.

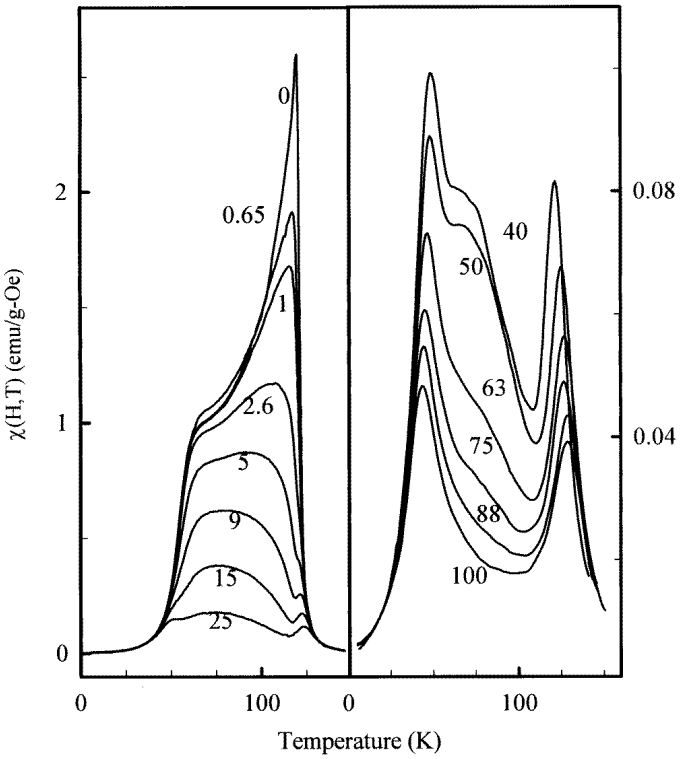

Figure 4. The temperature dependence of the field-dependent ac susceptibility $\chi(H, T)$ (in emu g^{-1} Oe^{-1}), corrected for background and demagnetizing effects, of the $x = 0.30$ sample. The numbers marked against each curve indicate the applied field H_a (in Oe).

4. The field-dependent response

4.1. The upper transition

Figures 4 and 5 demonstrate that as the applied field H_a increases, so the principal (Hopkinson) maximum (near 115 K and 60 K respectively) is suppressed. As a consequence, secondary, critical peaks characteristic of a paramagnetic-to-ferromagnetic transition emerge near 120 K and 90 K respectively. Such peaks are displayed for the $x = 0.3$ sample in considerable detail in figure 6; with increasing field H_a the peak amplitude decreases while the peak temperature increases above T_c; the locus of these maxima delineates [6, 16, 17] the crossover line (the dotted line) separating the higher-temperature thermally dominated response from the lower-temperature field-dominated regime. While the occurrence of such a peak structure can be understood on the basis of the fluctuation-dissipation theorem [18], a quantitative analysis of such behaviour utilizes the well-established relationship between the singular component in $\chi(H, T)$ and the usual linear scaling fields $t = (T - T_c)/T_c$ and $h \sim H_i/T$ given by the static scaling law [6, 19]

$$\chi(h, t) = t^{-\gamma} F\left(\frac{h}{t^{\gamma+\beta}}\right) = h^{1-1/\delta} G\left(\frac{h}{t^{\gamma+\beta}}\right). \tag{1}$$

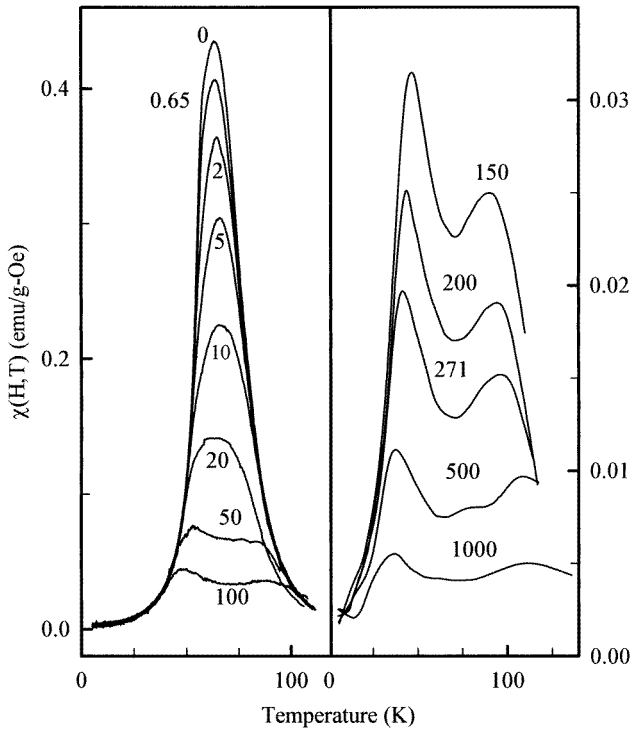

Figure 5. As figure 4, but for the $x = 0.32$ sample.

From this one predicts that the temperatures T_m of the susceptibility maxima increase with increasing field according to

$$t_m = \left(\frac{T_m - T_c}{T_c}\right) \propto H_i^{1/(\gamma+\beta)} \tag{2}$$

(the locus of the crossover line), while the peak amplitude decreases as the field increases; that is,

$$\chi(H_i, T_m) \propto H_i^{1/\delta-1}. \tag{3}$$

Both variations are in agreement with the experimental trends. These latter two equations and that governing the evolution of the effective Kouvel–Fisher susceptibility exponent [20]

$$\gamma^*(t) = \mathrm{d}[\ln \chi(0, t)]/\mathrm{d}[\ln(t)] \tag{4}$$

form the basis of a more detailed analysis, as outlined previously [6, 16], including the iterative procedure by means of which a first estimate for T_c is obtained, and subsequently refined.

Figures 7 and 8 provide a comparison between $\chi(H, T)$ measured for both samples in the vicinity of the upper transition with the power-law predictions of equations (2) and (3). In the case of the $x = 0.30$ specimen, both sets of data are *consistent* with *asymptotic* exponent values given by the isotropic three-dimensional Heisenberg model [21] ($\delta = 4.80$ and $\gamma + \beta = 1.75$). From figure 7 one obtains $\delta = 4.86 \pm 0.03$ for $14 \leqslant H_i \leqslant 10^3$ Oe (with the internal field $H_i = H_a - NM$ estimated using a previously outlined method [6, 16]), while from figure 8 one obtains $\gamma + \beta = 1.75 \pm 0.13$ for $14 \leqslant H_i \leqslant 10^2$ Oe

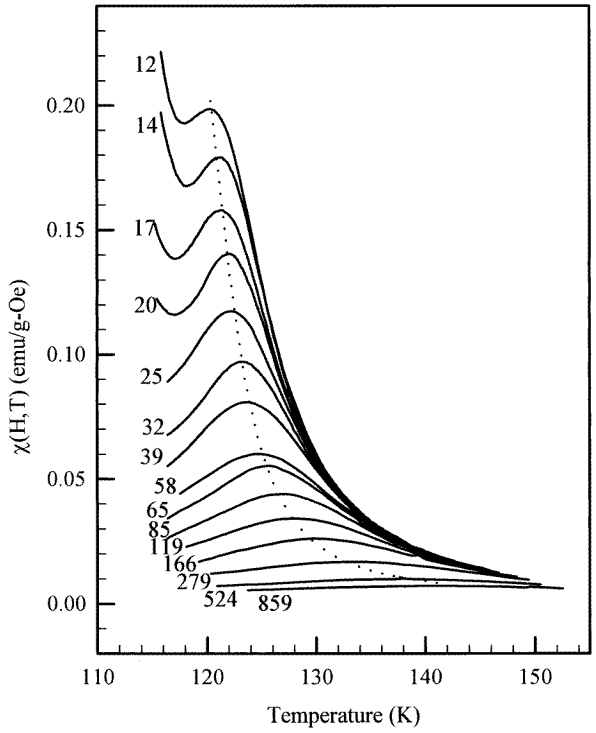

Figure 6. The detailed behaviour of the field-dependent ac susceptibility $\chi(H, T)$ (in emu g^{-1} Oe^{-1}) for the $x = 0.30$ sample, corrected for background and demagnetizing effects, as a function of temperature in the vicinity of the paramagnetic-to-ferromagnetic transition (the higher-temperature feature in figure 4). The numbers marked against each curve are the corresponding applied fields H_a (in Oe). The locus of these critical maxima—the crossover line—is depicted as the dotted line.

(with $T_c = 118 \pm 0.2$ K). In this latter plot, however, deviations above such an asymptotic dependence are seen for $H_i > 10^2$ Oe (from equation (2)—a decreasing slope corresponds to increasing values of $\gamma^* + \beta^*$). Such deviations are not unexpected since *effective* γ^*- and β^*-values which increase with increasing field (as figure 8 suggests—see also figure 9 below) have been observed for many other systems [1, 6, 16], and such behaviour is predicted by some models incorporating exchange bond disorder [6, 17, 22]. What is unusual about the amorphous FeMn system is not the presence of such effects for the $x = 0.3$ sample in figure 8, but the absence of similar effects for the same sample over the same field range in figure 7. Specifically, an exchange-coupling distribution which *is* expected in this system and which leads to the behaviour for $\gamma^* + \beta^*$ discussed above should also lead to δ^*-values which decrease with increasing field [6, 16, 17, 22]; the latter is not observed. Parallel results were also reported previously for $x = 0.20$ and $x = 0.26$; while no detailed explanation for such behaviour exists currently, these data are not inconsistent with a Widom-like inequality amongst these *effective* exponents, $\gamma^* \geqslant \beta^*(\delta^* - 1)$, the validity of which would not require each exponent to have the same dependence on the field.

The data for the $x = 0.32$ specimen displays somewhat different characteristics. Figure 8 confirms that some of these data at this composition *are* consistent with model predictions [21] (the experimental uncertainty and limited field range notwithstanding), namely $\gamma + \beta =$

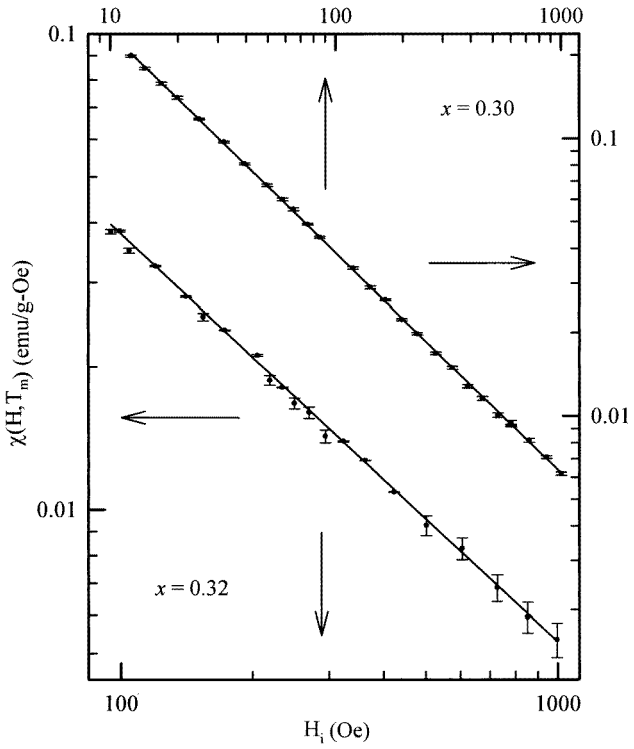

Figure 7. The critical peak amplitude $\chi(H, T_m)$ (in emu g^{-1} Oe^{-1}), corrected for background and demagnetizing effects and obtained from data similar to those shown in figure 6, plotted against the estimated internal field H_i (in Oe) (see the text) for both $x = 0.30$ and $x = 0.32$. The solid lines confirm the power-law prediction for $\chi(H_i, T_m)$—equation (3)—and yield the values of the exponent (δ) discussed in the text.

$1.7(5) \pm 0.3$ for $10^2 \leqslant H_i \leqslant 10^3$ Oe (with $T_c = 78.2 \pm 0.9$ K), while others shown in figure 7, are *not*. The latter figure confirms the power-law prediction of equation (3) with a unique exponent value over the limited field range ($10^2 \leqslant H_i \leqslant 10^3$ Oe) for which the critical peaks are well resolved, but the associated exponent value, $\delta^* = 7.0 \pm 0.1$, is far removed from model predictions. While it might be suggested that if these critical peaks could be resolved in lower fields ($H_i \leqslant 10^2$ Oe) they *might* reveal a trend towards the expected asymptotic value, a close examination of these data indicates little sign of the associated exponent estimate either increasing or decreasing with field over the available range. Furthermore, while model calculations yield field-dependent effective δ^* values, the latter are predicted, and almost invariably are observed, to *decrease* with *increasing* field from an appropriate model value near $H_i = 0$ (a result mentioned in a previous discussion [1] of the behaviour of an $x = 0.235$ sample). Here δ^* far *exceeds* model value estimates, rather than underestimating them. Currently we have no quantitatively satisfactory explanation for this behaviour; nevertheless we suggest that it may reflect the proximity of this composition to the so-called tricritical point [3]. Specifically, the failure of low applied fields to resolve the critical peak structure (as occurs for this sample) is usually attributed [6, 16] to the presence of considerable coercivity, so the singular contribution to the response does not dominate the regular/technical contribution over the corresponding field range. On qualitative grounds, significant coercivity/irreversibility is expected to emerge near the

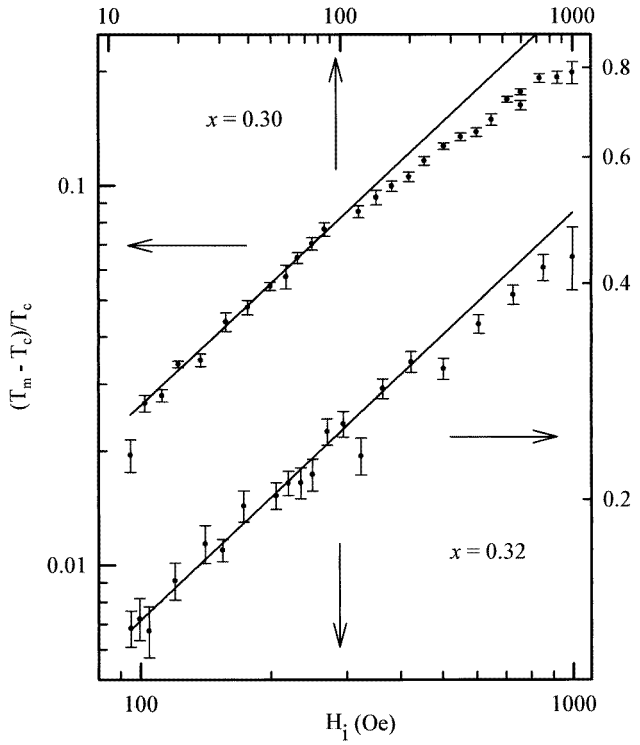

Figure 8. The (reduced) critical peak temperature t_m $(=(T_m - T_c)/T_c)$ plotted against the estimated internal field H_i (in Oe) for the $x = 0.30$ and $x = 0.32$ specimens. The solid lines indicate the power-law dependence, equation (2), and yield the values of $\gamma + \beta$ discussed in the text.

critical composition for the appearance of a frustrated (spin-glass) ground state.

Despite the reservations discussed above, confirmation that both samples do possess considerable exchange bond disorder is provided by the temperature dependence of the effective susceptibility exponent $\gamma^*(T)$ reproduced in figure 9. The non-monotonic variation evident there—in particular the appearance of a maximum above T_c—is a characteristic feature of such disorder, well documented previously [23]. Thus the upper transition at these compositions exhibits well-defined features characteristic of a continuous paramagnetic-to-ferromagnetic phase change. While there are some complications in the behaviour of $\delta^*(H)$ at $x = 0.32$, this response overall is consistent with Heisenberg model exponents *at* the critical point, with clear evidence for the influence of the (expected) variance in the distribution of exchange couplings *away* from this point.

4.2. The lower transition

4.2.1. The low-temperature peak. As is evident from the higher-field data in figures 4 and 5, with increasing H_a the principal (Hopkinson) maximum (the location of which is determined by technical/regular considerations, *not* critical fluctuations) in $\chi(H, T)$ is suppressed, and this enables a double-peaked structure to be identified (this requires fields >25 Oe for the $x = 0.30$ sample, and >50 Oe for $x = 0.32$). Such a double-peaked structure is consistent with Ising model predictions [6, 9], as is the evolution of these peaks

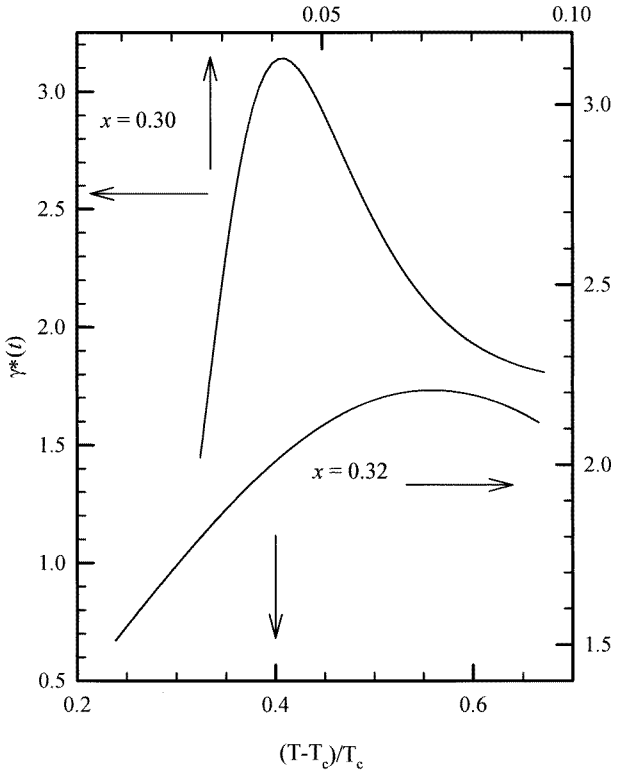

Figure 9. The effective Kouvel–Fisher susceptibility exponent $\gamma^*(t)$—equation (4)—plotted against reduced temperature for the $x = 0.30$ and $x = 0.32$ samples.

with field; the lower peak moves downwards and the upper peak increases in temperature as H_a increases, while the lower (potentially re-entrant) peak height exceeds the upper (ferromagnetic) peak amplitude in a given field. While vector models, unlike their Ising counterparts, do *not* predict a double-peaked structure in $\chi(H, T)$, such low-temperature features have, nevertheless, frequently been compared with vector model predictions, as vector model approaches are seen as being generally less restrictive than Ising theories. Vector models, as mentioned in the introduction, predict two low-temperature features accompanying re-entrant behaviour, the GT line (generally the higher-temperature feature) and the AT line. Such features are predicted to display different field dependences, and here we first consider the possibility that the lower-temperature peaks observed in the experimental data can be associated with either 'line'.

Near the multicritical point (at which the ferromagnetic and the re-entrant spin-glass phase boundaries are predicted to meet), the field dependence of the GT line is given by [24]

$$T_{\mathrm{GT}}(0) - T_{\mathrm{GT}}(H) = \sqrt{2}\left[\frac{m^2 + 4m + 2}{4(m+2)^2}\right]\frac{g\mu_{\mathrm{B}}H}{k_{\mathrm{B}}} \tag{5}$$

where m is the spin dimensionality and the other symbols assume their usual meaning.

With $T_{\mathrm{GT}}(H)$ identified with the lower-peak temperatures—shown in more detail for the $x = 0.32$ sample in figure 10—a comparison between similar data for $x = 0.30$ and equation (5) is effected in figure 11. For the field range over which such peaks are resolved,

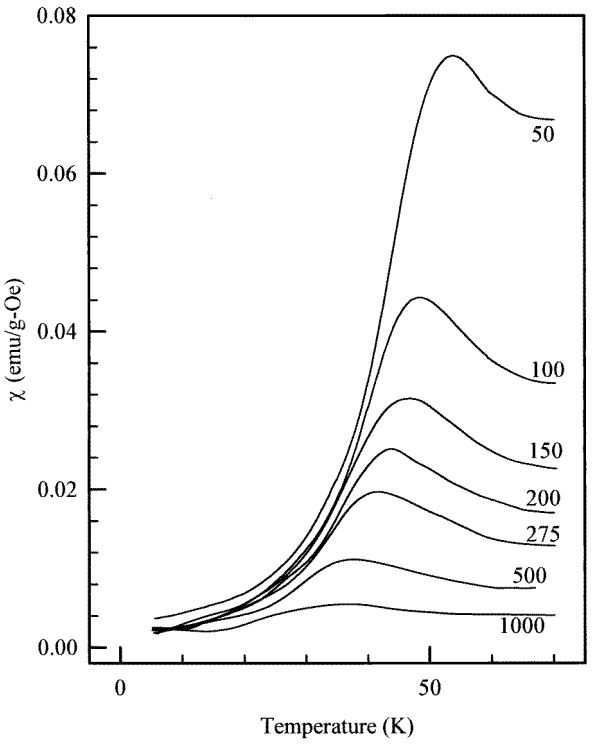

Figure 10. The detailed field-dependent ac susceptibility $\chi(H, T)$ (in emu g^{-1} Oe^{-1}) (corrected for background and demagnetizing effects) of the $x = 0.32$ sample in the low-temperature region. The corresponding static applied fields, H_a (in Oe), are marked against each curve.

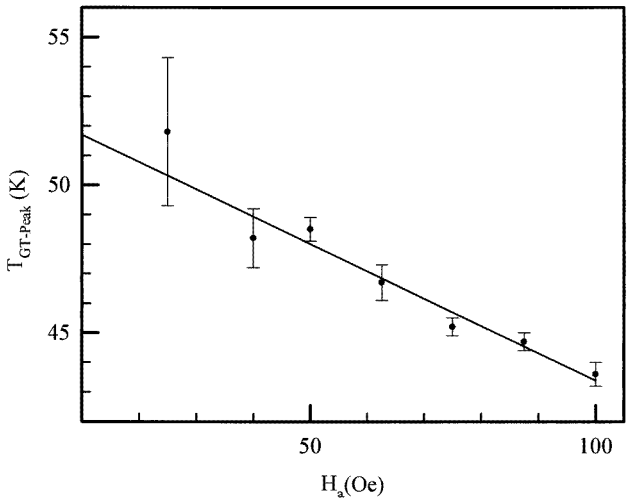

Figure 11. The estimated (lower-) peak temperature (designated T_{GT} (in K)), taken from data similar to those shown in figure 10, for the $x = 0.30$ sample, plotted against the corresponding applied field H_a (in Oe). The straight line drawn is consistent with the linear field dependence contained in equation (5).

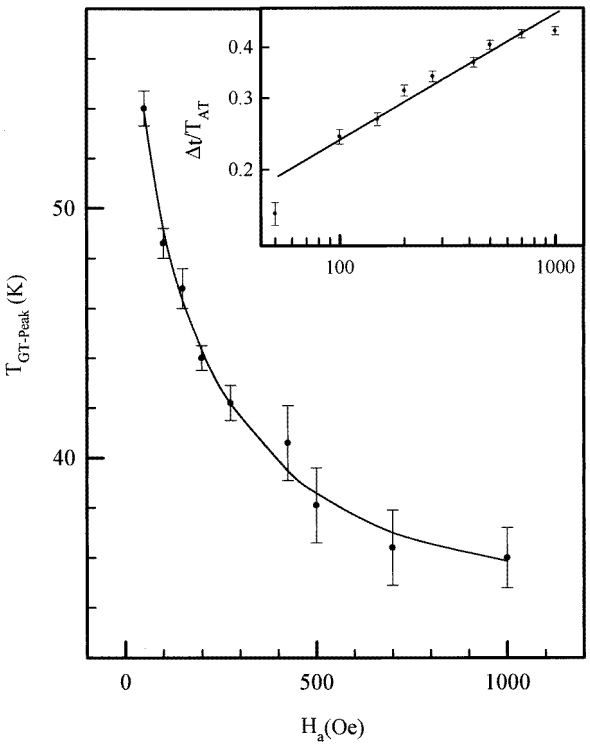

Figure 12. As figure 11, but for the $x = 0.32$ specimen; the line is drawn as a guide. The inset shows a comparison of these data with the behaviour predicted by equation (6) (see the text).

agreement *is* obtained between the predicted linear variation and available data for the $x = 0.30$ sample (the considerable experimental uncertainties notwithstanding) but *not* for the $x = 0.32$ specimen, as is evident from figure 12, despite the closer proximity of the latter sample to the multicritical point. This agreement for $x = 0.30$ is, however, fortuitous; while the linear variation is reproduced, these data exhibit a slope which exceeds the model value (equation (5) with $m = 3$) by a factor of at least 10^3. Similar comments apply to attempts to fit the *initial* variation of the data for $x = 0.32$ to the same expression. Such considerations argue against the association of this low-temperature peak in $\chi(H, T)$ for these samples with the location of the GT line.

Furthermore, while the line drawn through the data for $x = 0.32$ in figure 12 is just a guide, not a model fit, it does incorporate features attributable possibly to the AT line, the lower-temperature features of vector models. The latter is believed [4] to approach zero field with progressively increasing slope:

$$\frac{T_{\mathrm{AT}}(0) - T_{\mathrm{AT}}(H)}{T_{\mathrm{AT}}(0)} = \left(\frac{3}{4}\right)^{1/3}\left[\frac{g\mu_{\mathrm{B}}H}{k_{\mathrm{B}}T_{\mathrm{AT}}(0)}\right]^{n} \tag{6}$$

with $n < 1$. Such a power-law prediction is examined in the inset in figure 12, from which it is evident that such a form does not yield a convincing fit. A close examination of the data in this inset reveals continuous curvature, rather than the straight line expected for such a power-law dependence displayed on a double-logarithmic scale. Furthermore, the line drawn corresponds to a value of $n \simeq 0.3$, less than half the mean-field prediction [7] of 2/3 and significantly smaller than Monte Carlo estimates [25] of 0.55–0.7, so such a

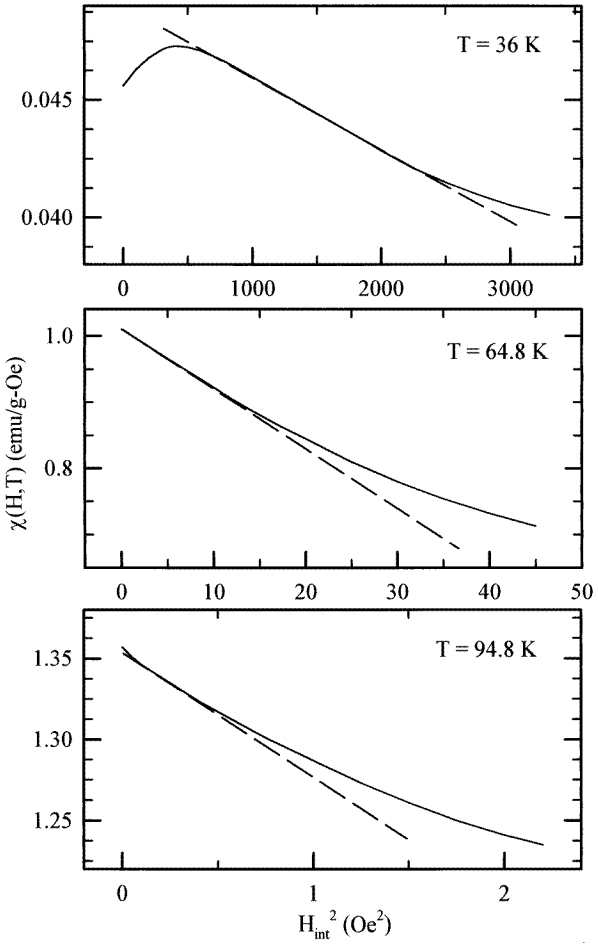

Figure 13. The continuously recorded field-dependent ac susceptibility $\chi(H, T)$ for the $x = 0.30$ sample (in emu g^{-1} Oe^{-1}, corrected for background and demagnetizing effects) plotted against the square of the estimated internal field H_i (in Oe), for three representative temperatures. The dashed lines provide estimates for the coefficient $a_2(T)$ in equation (7) (see the text).

dependence has no direct interpretation, at least within the framework of current models. In addition, the line drawn in the inset corresponds to a prefactor some three to four times larger than that predicted in equation (6). All of the latter mimic the situation reported previously for $x = 0.235$ and 0.26. Indeed, to reiterate points made with respect to these latter samples in this context, the curvature evident in the inset in figure 12 could be reduced by increasing $T_{AT}(0)$ above the value of 64 K used in constructing this figure, but this would cause the estimate for n to depart even further from predicted values; decreasing $T_{AT}(0)$ to increase n towards model estimates (at least when deduced from higher-field points) would accentuate the low-field deviations. The values indicated for n and $T_{AT}(0)$ thus reflect an overall compromise. Nevertheless the analysis and discussion presented above suggest that the low-temperature peak structure does *not* conform with vector model predictions for either the GT or the AT line, a conclusion in agreement with that reported earlier for the $x = 0.235$ and $x = 0.26$ samples [1].

4.2.2. Non-linear susceptibility. By contrast, the behaviour of the non-linear response in the low-temperature regime does not rule out the possibility of a re-entrant transition. This conclusion is reached through an examination of the temperature dependence of $a_2(T)$, the coefficient characterizing the lowest field-dependent term in $\chi(H, T)$; that is, the latter can be written as (since the magnetization in these systems is an odd function of field, i.e. it reverses when the field reverses, the susceptibility can only depend on even powers of the field):

$$\chi(H, T) = \chi(0, T) - a_2(T)H^2 + a_4(T)H^4 - \cdots \tag{7}$$

and the corresponding $a_2(T)$ value found from the asymptotic ($H \to 0$) slope of $\chi(H, T)$ versus H^2 plots at various fixed temperatures. The coefficient $a_2(T)$ found in this way has been shown to display a marked increase as the re-entrant boundary is approached from below for systems like amorphous **Fe**Zr and (**Pd**Fe)Mn; in addition, this coefficient [26] also diverges (as $t^{-3\gamma+2\beta}$) near the ferromagnetic ordering temperature T_c. Such a double-peaked structure in the temperature dependence of $a_2(T)$ agrees qualitatively with Ising model predictions [6, 9] (although the exponent values are expected, and observed, to be different).

Having presented a comprehensive selection of similar plots previously [6, 10, 11] for a variety of systems, including [1] the present series with $x = 0.235$ and $x = 0.26$, here we reproduce a limited selection of representative data for $x = 0.30$. Figure 13 displays such plots for temperatures of 36, 65 and 95 K, i.e. just below and just above T_{xy}, and near T_c for this sample. The influence of a significant coercive field is evident only at temperatures well below T_{xy} (<40 K here) where—despite excluding fields below $H_c(T)$ in estimating $a_2(T)$ and thus setting an upper limit on the latter—the leading non-linear contribution remains small. This figure also verifies the alternating negative and positive signs for the contributions to $\chi(H, T)$ made by terms involving $a_2(T), a_4(T)$, etc (through the sign of the deviations away from the initial H^2-behaviour), and confirms another Ising model result that as the magnitude of $a_2(T)$ increases so the range of field over which $\chi(H, T)$ is dominated by the $a_2(T)H^2$ component falls (as terms in $a_4(T)H^4$ and $a_6(T)H^6$, etc, play an increasingly important role).

Figure 14 summarizes the temperature dependence of the coefficient $a_2(T)$, so obtained, for the $x = 0.30$ and $x = 0.32$ specimens. Contrary to the conclusions reached above following comparisons with vector model predictions, the double-peaked structure evident in this figure *is* consistent with the qualitative—if not the quantitative—behaviour expected for this coefficient in systems undergoing sequential magnetic transitions. For $x = 0.30$ the temperature dependence of $a_2(T)$ is reminiscent of that observed [10] for amorphous $Fe_{1-x}Zr_x$ with $x = 0.08$ and 0.09; namely while the critical behaviour near the paramagnetic-to-ferromagnetic transition ($T_c = 118$ K) is well defined (as discussed above) and $a_2(T)$ exhibits a marked increase near T_c (with more careful studies on other systems showing [26] an actual divergence as $t^{-3\gamma+2\beta}$), the lower-temperature anomaly is less pronounced. This latter anomaly is clearly not divergent and is thus significantly weaker than Ising model predictions. Diverging anomalies in the non-linear response provide the principal evidence for characterizing the *direct* paramagnetic–spin-glass transition as a true thermodynamic phase change. The latter is, however, known to be complicated by the severe effects of critical slowing down [4, 5] (the corresponding exponent $z\nu$ can exceed 10), and similar effects are expected to be present at the ferromagnet-to-(transverse) spin-glass re-entrant transition. The dynamic nature of the current measurements may be quite constrained by such effects (which could lead to a marked 'rounding' of $a_2(T)$). Of comparable concern is the limitation of the dimensionality of the Ising approach, which is unlikely

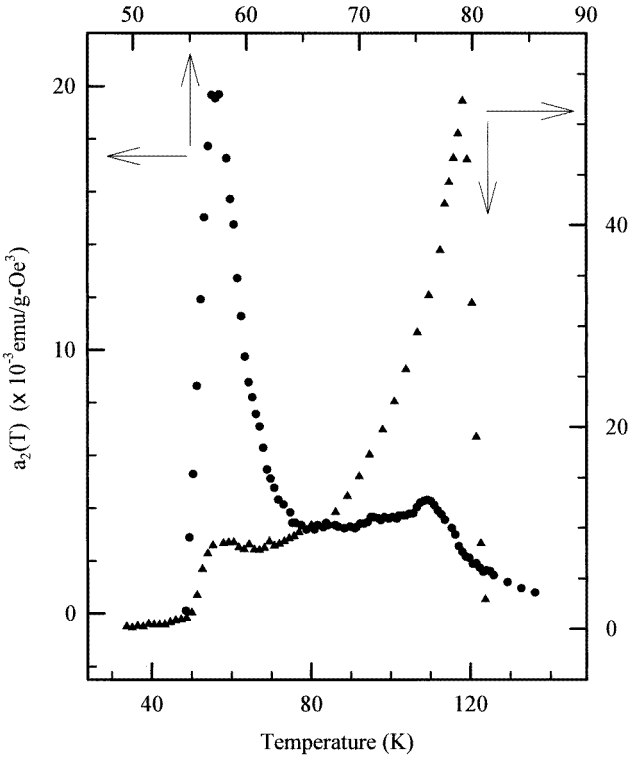

Figure 14. The coefficient $a_2(T)$ (in 10^{-3} emu g^{-1} Oe^{-3}) of equation (7), estimated from data similar to those shown in figure 13, plotted against temperature for the $x = 0.30$ (▲) and the $x = 0.32$ (●) samples.

to predict correctly the (possibly weak) coupling between the transverse spin freezing and the (measured) longitudinal response [27].

For the $x = 0.32$ specimen the apparent strength of these anomalies is reversed; that occurring near $T_{xy} \sim 57$ K is more marked than that near $T_c \sim 76$ K. To our knowledge this is the first time that such a 'reversal' has been observed. While similar reservations remain regarding constraints related to the use of dynamical probes (which appear to eventually underestimate the true response no matter how low the measuring frequency) and the strength of the transverse-to-longitudinal coupling, two anomalies in $a_2(T)$ are present. Furthermore, while there is no theoretical explanation currently for the changing amplitude of the peaks in $a_2(T)$, we suggest that the proximity of the $x = 0.32$ sample to the multicritical point may play a significant role.

Thus, the behaviour of the coefficient $a_2(T)$ *is*, at least, consistent with a second ferromagnet-to-(transverse) spin-glass transition, unlike other features related to vector model approaches.

5. Summary and conclusions

Features present in both the zero-field and the field-dependent susceptibility, $\chi(H, T)$, of $(Fe_{1-x}Mn_x)_{75}P_{16}B_6Al_3$ for $x = 0.30$ and 0.32 are qualitatively consistent with the presence of sequential, re-entrant behaviour. Specifically, detailed analysis of such data for

$x = 0.30$ confirms the presence of a paramagnetic-to-ferromagnetic phase transition (with Heisenberg model exponents) and a double-peaked structure in the temperature dependence of the coefficient $a_2(T)$. For $x = 0.32$, characteristics consistent with those expected in $\chi(H, T)$ near a crossover line associated with a paramagnetic-to-ferromagnetic transition are observed, along with a double-peaked structure in the variation of $a_2(T)$ with temperature. In the latter system, however, both exponent values deduced near T_c and the relative amplitudes of $a_2(T)$ near T_c and T_{xy} are anomalous, a result (qualitatively) attributed to the proximity of this composition to the paramagnetic–ferromagnetic–(transverse) spin-glass multicritical point.

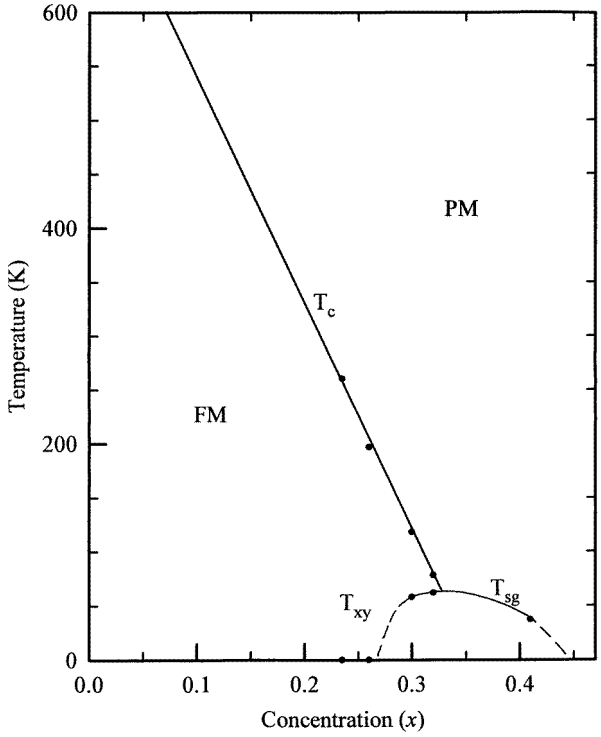

Figure 15. The modified phase diagram suggested for $(Fe_{1-x}Mn_x)_{75}P_{16}B_6Al_3$.

While these data provide quantitative support for previous conclusions regarding the possible occurrence of sequential phase transitions at these compositions, when combined with earlier field-dependent ac susceptibility data and their analysis, they suggest a modified phase diagram—figure 15. Here the potentially re-entrant boundary falls to zero temperature below $x = 0.30$, so for $x = 0.26$ (and below) only a paramagnetic-to-ferromagnetic transition is exhibited on cooling.

Acknowledgments

It is a pleasure to thank Dr I Mirebeau (Saclay), for the loan of the samples used in this study, and the Natural Sciences and Engineering Research Council (NSERC) of Canada for support in terms of both operating grants (to GW) and postgraduate fellowships (to AGB).

References

[1] Berndt A G, Chen X, Kunkel H P and Williams G 1995 *Phys. Rev.* B **52** 10 160
[2] Senoussi S, Hajoudj S and Fourmeaux R 1988 *Phys. Rev. Lett.* **61** 1013
[3] Mirebeau I, Itoh S, Mitsuda S, Watanabe T, Endoh Y, Hennion M and Papoular R 1990 *Phys. Rev.* B **41** 11 405
[4] Binder K and Young A P 1986 *Rev. Mod. Phys.* **58** 801
[5] Hertz J and Fischer K A 1989 *Spin Glasses* (New York: Cambridge University Press)
[6] Williams G 1991 *Magnetic Susceptibility of Superconductors and Other Spin Systems* ed R A Hein *et al* (New York: Plenum)
[7] Gabay M and Toulouse G 1981 *Phys. Rev. Lett.* **47** 201
[8] de Almeida J R L and Thouless D J 1978 *J. Phys. A: Math. Gen.* **11** 983
[9] Kornik K, Roshko R M and Williams G 1989 *J. Magn. Magn. Mater.* **81** 323
[10] Ma H, Kunkel H P and Williams G 1992 *J. Phys.: Condens. Matter* **4** 1993
[11] Kunkel H P and Williams G 1988 *J. Magn. Magn. Mater.* **75** 98
[12] Fiorani D, Dormann J L, Tholence J L, Bessais L and Villers D 1986 *J. Magn. Magn. Mater.* **54–57** 173
[13] Aeppli G, Shapiro S M, Birgeneau R J and Chen H S 1983 *Phys. Rev.* B **28** 5160
Aeppli G, Shapiro S M, Birgeneau R J and Chen H S 1984 *Phys. Rev.* B **29** 2589
[14] Maartense I 1970 *Rev. Sci. Instrum.* **41** 657
[15] Osborn T A 1945 *Phys. Rev.* **67** 351
[16] Wang Z, Kunkel H P and Williams G 1992 *J. Phys.: Condens. Matter* **4** 10 385
Ho S C, Maartense I and Williams G 1981 *J. Phys. F: Met. Phys.* **11** 699
[17] Roshko R M and Williams G 1984 *J. Phys. F: Met. Phys.* **14** 703
[18] Kunkel H P, Roshko R M and Williams G 1988 *Phys. Rev.* B **37** 5880
[19] Stanley H E 1971 *Introduction to Phase Transitions and Critical Phenomena* (Oxford: Clarendon)
[20] Kouvel J S and Fisher M E 1964 *Phys. Rev.* **136** A1626
[21] LeGuillou L C and Zinn-Justin J 1980 *Phys. Rev.* B **21** 3976
[22] Kornik K, Kunkel H P, Roshko R M and Williams G 1990 *Solid State Commun.* **76** 993
[23] Kaul S N 1985 *J. Magn. Magn. Mater.* **53** 5
[24] Dubiel S M, Fischer K, Sauer Ch and Zinn W 1987 *Phys. Rev.* B **36** 360
[25] Bhatt R N and Young A P 1985 *Phys. Rev. Lett.* **54** 924
[26] Kunkel H P and Williams G 1988 *J. Phys. F: Met. Phys.* **18** 1271
[27] Katori M and Suzuki M 1985 *Prog. Theor. Phys.* **74** 1175